Indonesian Journal of Electrical Engineering and Computer Science
Vol. 42, No. 1, April 2026, pp. 13~22
ISSN: 2502-4752, DOI: 10.11591/ijeecs.v42.i1.pp13-22

Characteristics dipole antenna for partial discharge in gas insulated switchgear

Rian Nurdiansyah[1], Farradita Nugraha[1], Nadya Glaudira[1], Linda Faridah[1,2]
[1]Department of Electrical Engineering, Faculty of Engineering, Universitas Siliwangi, Tasikmalaya, Indonesia
[2]Universitas Negeri Yogyakarta, Yogyakarta, Indonesia

Article Info

Article history:

Received Nov 20, 2025
Revised Jan 28, 2026
Accepted Mar 4, 2026

Keywords:

Dipole antenna
Gas insulated switchgear
High voltage measurement
Partial discharge
Ultra-high frequency

ABSTRACT

The insulation condition of high-voltage equipment can be determined by measuring partial discharge (PD), which is an important indicator in insulation degradation. One of the PD detection methods that can be used is to use antennas as sensors in detecting electromagnetic waves generated from PD activities, especially in gas insulated switchgear (GIS) systems. This study focuses on designing and testing dipole antennas in the ultra-high frequency (UHF) frequency range of 300 Mhz-3 GHz to detect PD signals in GIS. Previous studies on dipole antennas with dimensions of 66×15 mm have reported a bandwidth of 336 MHz and a return loss of -22.4 dB at 1.3 GHz. The antenna was fabricated using an FR4-epoxy substrate with a thickness of 1.6 mm, a substrate radius of 102 mm, and a gap distance of 2 mm. Optimization of the antenna length and width significantly improved performance characteristics. Simulation results show that a dipole antenna with dimensions of 35×40 mm antenna produced a wider bandwidth of 989 MHz with a return loss of −28.47 dB at 1.4 GHz. Experimental validation using vector network analyzer (VNA) and PD testing on GIS confirmed that the optimized dipole antenna effectively detected PD activity at a voltage level of 16 kV.

Corresponding Author:

Farradita Nugraha
Department of Electrical Engineering, Faculty of Engineering, Universitas Siliwangi
46115 Tasikmalaya, Jawa Barat, Indonesia
Email: farraditanugraha@unsil.ac.id

1. INTRODUCTION

The insulation condition of high-voltage equipment is commonly assessed through partial discharge measurements. Antenna sensors, which detect electromagnetic waves generated by partial discharge activity, are commonly used in gas-insulated switchgear [1], [2]. The range of frequency from 300 MHz to 3 GHz, classified as ultra-high frequencies (UHF), represents the electromagnetic wave signals utilized in GIS [3], [4]. Electromagnetic waves can be measured using UHF antennas [5]. Compared to gas sensors, UHF sensors in gas-insulated switchgear (GIS) offer faster response times and higher sensitivity [6]. The UHF method operates within a frequency range of 300 MHz to 3 GHz in GIS. An antenna designed for this frequency range effectively detects partial discharge, confirming its suitability for GIS monitoring.

UHF antennas employed as sensors for partial discharge (PD) detection must exhibit high sensitivity and a broad bandwidth. Furthermore, the antenna dimensions should correspond to the opening window in the GIS. Optimization of antenna design should consider the specific parameters required by the PD sensor [7].

Important parameters for antennas employed as sensors include bandwidth and return loss. Bandwidth is generally defined as the range of frequencies within the UHF band where the return loss (RL) value remains below -10 decibels (dB). This criterion is widely used for bandwidth calculation in most studies [8]-[13].

Antennas operate by receiving and transmitting electromagnetic signals. A dipole antenna features a symmetrical structure, with both sections exhibiting identical shapes and dimensions. The length and width of dipole antennas may be modified to accommodate particular applications.

The antenna design process typically begins with the use of three-dimensional modeling software, such as HFSS [14]. Subsequent stages involve testing with a vector network analyzer (VNA) and assessing the antenna's performance as a sensor for detecting partial discharge in GIS [15], [16]. In this study, dipole antennas were fabricated using three-dimensional modeling software, such as ANSYS HFSS, then tested with a VNA, and evaluated within GIS environments.

Dipole antennas are commonly employed to detect partial discharge [17]. A dipole antenna measuring 66 mm × 15 mm has previously been utilized to identify partial discharge in a 66 kV GIS model [18]. Table 1 shows the result of the dipole antenna at 66×15 mm.

Table 1. Simulated results of dipole antenna at 66×15 mm [18]

Name of antenna	Return Loss (dB)	Fr (GHz)	Bandwidth (MHz)
Dipole antenna	-22.4	1.3	336

Research on dipole antennas used as sensors has been limited. However, to date, dipole antennas have not been fabricated using three-dimensional modeling techniques that involve modifying antenna dimensions to optimize performance characteristics. The fabrication of dipole antennas with three-dimensional modeling aims to achieve optimal bandwidth, return loss, and resonance frequency, which are critical for effective partial discharge detection. In this context, the antenna's length and width are systematically varied to evaluate their impact on performance parameters.

2. OBJECTIVES

This study aims to design and analyze antennas operating within the 300 MHz to 3 GHz frequency range by varying key antenna parameters. Additionally, PD detection on GIS is evaluated using a dipole antenna as the sensor. This research contributes by proposing a method to determine optimal specifications for a dipole antenna, which has not been widely studied. Therefore, the author seeks to understand more deeply the changes that can be made to the dipole antenna's shape (length and width) to achieve the most effective antenna size. The determination of an antenna can be seen in its wide bandwidth, low return loss, and resonance frequency. Meanwhile, the antenna made is a microstrip patch antenna using FR4-epoxy substrate with a thickness of 1.6 mm, a substrate radius of 102 mm, and a gap distance of 2 mm.

3. METHOD

The fabrication of the dipole antenna begins with designing the antenna using three-dimensional modeling software. Following the identification of the optimal configuration, the antenna undergoes testing with a VNA. Subsequently, the antenna functions as a sensor for detecting partial discharge within the GIS [18]. The experimental procedure employed in this study is illustrated in Figure 1.

Figure 1 illustrates the methodology employed in this study. The process begins with specifying the desired antenna. First, a dipole antenna is designed as a microstrip patch antenna using an FR4-epoxy substrate with a thickness of 1.6 mm, a substrate radius of 102 mm, and a gap distance of 2 mm. Next, antenna simulations are conducted by varying the length and width parameters. Based on these simulation results, the optimal antenna is selected based on the criteria of wide bandwidth, low return loss, and resonant frequency. The selected antenna is then fabricated. After fabrication, a VNA is used to perform a measurement. Finally, the procedure concludes with PD testing, which represents the final stage of the research method.

A dipole antenna consists of two square plates arranged in series, each with identical dimensions and separated by a specified distance [19]. The square geometry is defined by its length (L) and width (W). Adjusting these parameters influences the resonance frequency, bandwidth, and return loss of the antenna.

The UHF response of dipole antennas is characterized by the following equations [18].

$$f_r = \frac{1}{2} \cdot k \cdot \frac{c}{l} \quad (1)$$

Where the f_r= resonant frequency of the antenna; k = constant 0.95; c = speed of light, 3×10^8 m/s; l = antenna length.

The expression for effective dielectric constant [20]:

$$\varepsilon_{eff} = \frac{\varepsilon_r+1}{2} + \frac{(\varepsilon_r-1)\left(1+12\frac{h}{W}\right)^{-1/2}}{2} \quad (2)$$

Where the ε_{eff} = effective dielectric constant; ε_r= dielectric coefficient; W= width of antenna; h = thickness of substrate.

The resonance frequency is given by [20].

$$f_r = \frac{c}{2(L+2\Delta L)\sqrt{\varepsilon_{eff}}} \quad (3)$$

Where, f_r= resonance frequency; c = speed of light, 3×10^8 m/s; L= length of antenna.

Dipole antennas are fabricated using three-dimensional imaging software. Figure 2 presents the results of the dipole antenna simulation.

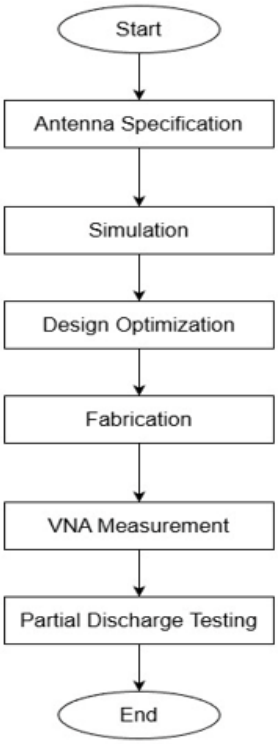

Figure 1. Research method flowchart

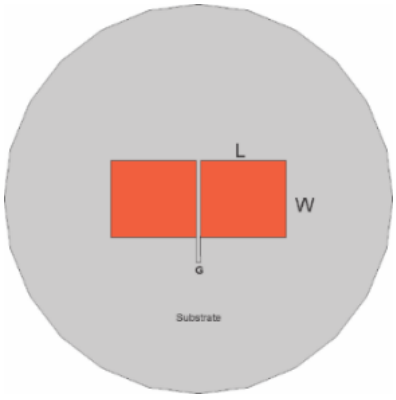

Figure 2. Dipole antenna configuration

Figure 2 illustrates the configuration of the dipole antenna. The performance of a dipole antenna is significantly influenced by its length and width. A gap exists between the two antenna elements, and a substrate serves as the material supporting the antenna patch. The primary design parameters in this study are the variations in width and length of the dipole antenna.

Following the simulation, the optimal antenna design is fabricated. To verify compliance with design specifications and optimal performance at the target frequency, the antenna is evaluated using a VNA. This evaluation measures electromagnetic characteristics, including return loss, resonance frequency, bandwidth, and antenna impedance. The Cobalt Series C1220 VNA, which operates over a frequency range of 100 kHz to 20 GHz, is utilized for these measurements.

The PD sensor testing on GIS evaluates the capabilities of the UHF dipole antenna, designed to detect PD events [21], [22]. The GIS model employs SF_6 insulation for high-voltage applications and features specifications including a voltage rating of 36 kV, a current rating of 2000 A, a transient current rating of 25 kA for 3 seconds, and a gas pressure rating of 0.75 kgf/cm² [23], [24]. The model includes two circular windows, each with a diameter of 50 mm, for the placement of external sensors. A conductive shield within the GIS prevents electromagnetic waves from escaping. However, the presence of a window with insulating material allows signals from PD sources to be detected by external sensors. The dipole antenna is positioned outside the GIS, in close proximity to the GIS window.

4. RESULTS AND DISCUSSION

The following section presents the results of modifications to the dipole antenna's length and width, as well as the outcomes of antenna and PD sensor tests on the GIS.

4.1. Dipole antenna characteristics

The performance of a dipole antenna is significantly affected by its length and width. A gap exists between the two sections of the antenna, and a substrate supports the antenna patch [25]. This design specifically examines variations in the width and length of the dipole antenna.

4.1.1. Dipole antenna width change

In the width change, there are eight simulated sizes, including (D × L): 45×25 mm, 45×30 mm, 45×35 mm, 45×40 mm, 45×45 mm, 45×50 mm, 45×55 mm, and 45×60 mm. The Figure 3 shows the dipole antenna with Figure 3(a) sizes 45×30 mm and Figure 3(b) sizes 45×60 mm.

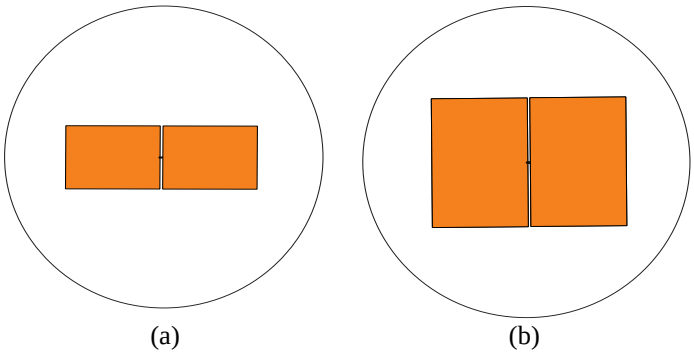

Figure 3. Dipole antenna (a) 45×30 mm and (b) 45×60 mm

For the width variation simulations, the following parameters were held constant: a FR4-epoxy substrate with a thickness of 1.6 mm, a substrate radius of 102 mm, a gap distance of 2 mm, and an antenna length of 45 mm. The simulation results for the effect of width variation on dipole antenna characteristics are presented in Table 2.

Simulation results for varying dipole antenna widths indicated that the configuration with the widest bandwidth, 819 MHz, occurred at a width of 45 mm and a length of 40 mm, accompanied by a return loss of -28.21 dB. For the voltage standing wave ratio (VSWR) simulation, the three optimal configurations were selected based on return loss and bandwidth: 45×35 mm, 45×40 mm, and 45×45 mm. The results of the top three impedance simulations for dipole antenna width variations are presented in Table 3.

Table 2. Simulated results of dipole antenna width variation on antenna characteristics

Size length × width (mm)	Return loss (dB)	Fr (GHz)	Bandwidth (MHz)
45×25	-22.81	1.2	368
45×30	-25.04	1.2	481
45×35	-25.30	1.2	619
45×40	-28.21	1.3	819
45×45	-23.15	1.3	784
45×50	-17.32	1.3	585
45×55	-15.22	1.3	515
45×60	-14.35	1.3	459

Table 3. Impedance simulation results for the three optimal dipole antenna width configurations

Size length×width (mm)	The impedance values for these configurations are close to 50 Ohms		
	Frequency 1 (GHz)	Frequency 2 (GHz)	Frequency 3 (GHz)
45×30	0.803	1.7	3.1
45×40	1.3	1.6	2.9
45×45	0.7	0.76	2.7

The VSWR is a parameter used to assess the degree of impedance matching between an antenna and the connected radio or transmission line. A VSWR value less than 2 is generally considered the standard for acceptable impedance matching 8,9,10,11,12,13. The three most effective impedance simulations demonstrate that varying the width of the dipole antenna produces three distinct operating frequencies with impedance values near 50 Ohms. According to the table, a dipole antenna measuring 45×30 mm achieves an impedance of 50 Ohms at 0.803 GHz, 1.7 GHz, and 3.1 GHz. For a dipole antenna sized 45×40 mm, the 50 Ω impedance occurs at 1.3 GHz, 1.6 GHz, and 2.9 GHz. In contrast, the 45×45 mm dipole antenna reaches 50 Ohms at 0.7 GHz, 0.76 GHz, and 2.7 GHz.

4.1.2. Dipole antenna length change

Six simulated dipole antenna sizes were evaluated for length variation, specifically (D × L): 25×40 mm, 30×40 mm, 35×40 mm, 40×40 mm, 45×40 mm, and 50×40 mm. In these simulations, the following parameters were held constant: FR4-epoxy substrate thickness of 1.6 mm, substrate radius of 102 mm, gap distance of 2 mm, and width of 40 mm. Figure 4 shows the sizes of 25×40 mm and 50×40 mm. The simulation results illustrating the effect of length variation on dipole antenna characteristics are presented in the Table 4.

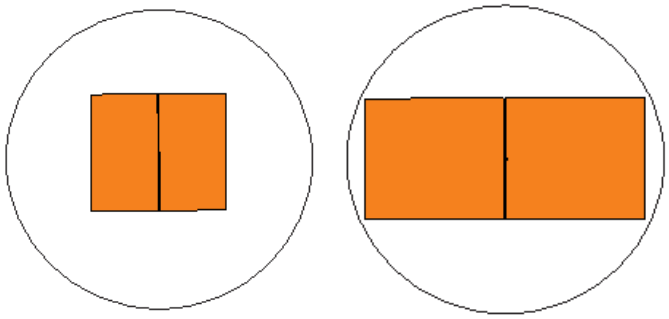

Figure 4. Dipole antenna (a) 25×40 mm and (b) 50×40 mm

Table 4. Simulation results for the effect of dipole antenna length variation on antenna characteristics

Size: length×width (mm)	Return loss (dB)	Frequency (GHz)	Bandwidth (MHz)
25×40	-22.06	1.3	436
30×40	-23.94	1.4	840
35×40	-28.47	1.4	989
40×40	-25.40	1.5	853
45×40	-28.21	1.3	819
50×40	-22.26	1.1	598

Simulation of dipole antenna length variations indicated that the 35×40 mm configuration achieved a minimum return loss of -28.47 dB at a resonance frequency of 1.4 GHz and a bandwidth of 989 MHz. For the voltage standing wave ratio (VSWR), values below 2 were observed for dipole antennas with dimensions of 30×40 mm, 35×40 mm, and 40×40 mm. The results of the three optimal impedance simulations for variations in dipole antenna length are presented in Table 5.

The data indicate that a dipole antenna measuring 30×40 mm exhibits an impedance of 50 ohms at 0.845 GHz. For a dipole antenna with dimensions of 35×40 mm, the 50-ohm impedance occurs at 0.846 GHz and 3 GHz. In contrast, the 45×40 mm dipole antenna achieves a 50-ohm impedance at 0.767 GHz, 1.6 GHz, and 2.932 GHz.

Based on variations in length and width, the three most effective antenna designs were selected. The optimal antenna simulations correspond to dimensions of 35×40 mm, 45×40 mm, and 45×45 mm.

Table 5. Simulation results for the three optimal dipole antenna length variations based on impedance performance

Size length×width (mm)	Impedance values that have a value close to 50 Ohms		
	Frequency 1 (GHz)	Frequency 2 (GHz)	Frequency 3 (GHz)
30×40	0,845		
35×40	0,846	3	
45×40	0,767	1,6	2,932

4.2. Dipole antenna simulation analysis

The performance of a dipole antenna is determined by parameters such as its width and length. This section presents an analysis of simulation results examining how variations in these dimensions affect the antenna's characteristics.

4.2.1. The effect of width variation

The width of the dipole antenna was varied in simulations from 45×25 mm to 45×60 mm, with increments of 5 mm between each configuration. Figure 5 shows how differences in antenna width affect the results. Specifically, Figure 5(a) presents the return loss values resulting from changes in width, while Figure 5(b) presents the bandwidth gain resulting from these changes. This sequence illustrates the impact of antenna width on both return loss and bandwidth gain.

As the width of the dipole antenna increases, the minimum return loss value also increases. The relationship between width and bandwidth is non-linear, with bandwidth exhibiting fluctuations as width changes. Optimal bandwidth and return loss are achieved at dimensions of 45 mm by 40 mm, indicating that the dipole antenna performs best at these specific widths.

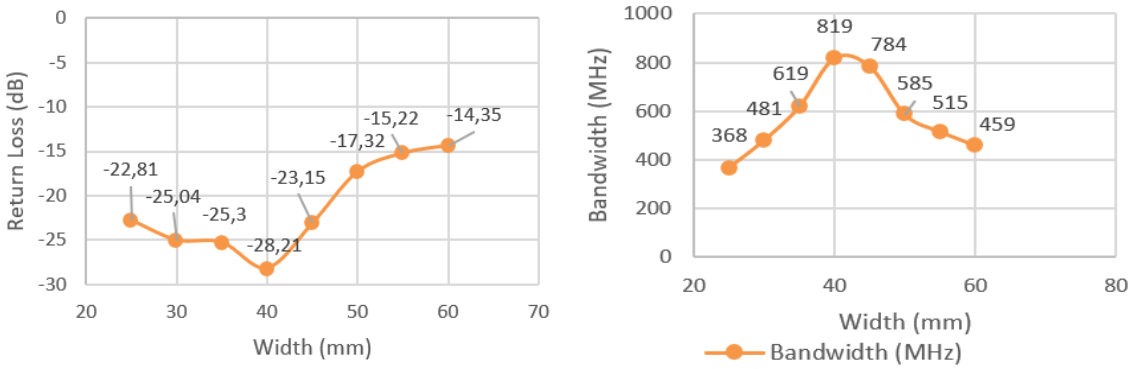

(a) (b)

Figure 5. Comparison of width variations on (a) return loss and (b) bandwidth

4.2.2. The effect of length variation

On dipole antennas, the simulation of length changes used is from 25×40 mm to 50×40 mm. Changes in antenna length, made from one size to the next size by 5 mm. Figure 6 demonstrates the impact of varying antenna length in three stages. Figure 6(a) presents the return loss for different lengths. Figure 6(b)

depicts the resonant frequency as a function of antenna length. Figure 6(c) illustrates the variation in bandwidth with respect to antenna length.

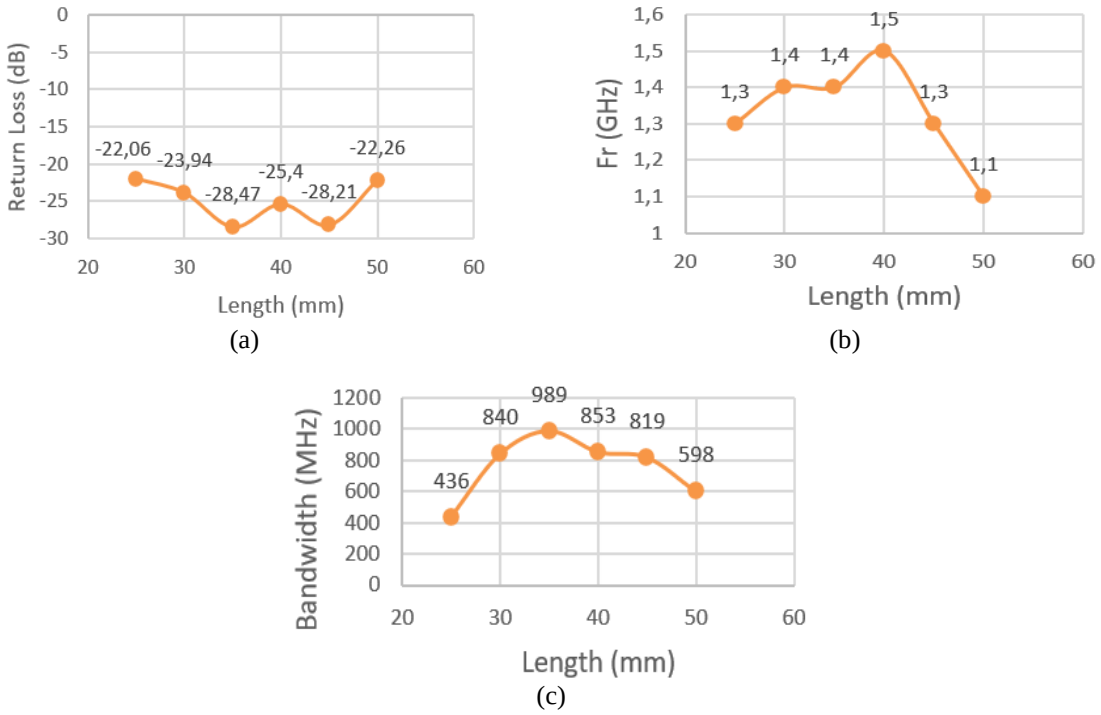

Figure 6. Comparison of the effects of length variation on (a) return loss, (b) resonance frequency, and (c) bandwidth

As the length of the dipole antenna increases, the resonance frequency decreases. Additionally, greater antenna length results in improved minimum return loss values. However, the bandwidth becomes more variable with increased length, with some lengths yielding larger bandwidths and others smaller. The UHF frequency response of a dipole antenna is determined by (1). By substituting different length values, such as 25 mm, 35 mm, and 45 mm, the following calculation results are obtained. Table 6 presents the results of simulations and calculations for antenna sizes of 25 mm, 35 mm, and 45 mm.

The results indicate that increasing the length of the dipole antenna leads to a decrease in the resonance frequency. Although the calculated and simulated values differ significantly, both methods demonstrate the same underlying principle: a longer dipole antenna produces a lower resonance frequency.

Optimizing dipole antenna performance requires adjusting its length. Reducing the antenna length increases the bandwidth, while increasing the length decreases the resonance frequency and reduces the return loss. Therefore, careful modification of the antenna length is essential to achieve the desired performance characteristics.

Table 6. Simulation and calculation results for variations in antenna length

Size length (mm)	Resonance frequency (GHz)	
	Simulation	Calculation
25	1,3	5,7
35	1,4	4,07
45	1,3	3,16

4.3. PD measurement results on GIS

Based on variations in length and width, the three most effective antennas were selected: 35×40 mm, 45×40 mm, and 45×45 mm. For the PD measurement in GIS, a dipole antenna with dimensions of 45×45 mm was utilized. PD test on solid insulation is one of the methods that determine the quality of insulation [26].

4.3.1. PDIV measurement

Partial discharge inception voltage (PDIV) is defined as the voltage at which partial discharge (PD) is first observed during the experiment. The voltage is gradually increased from a level where no PD is detected until PD appears. Measuring PDIV provides a reference for the minimum source voltage required to initiate PD in the test object. In this study, PDIV measurements were conducted using both the antenna sensor and the RC detector. Table 7 shows the results of the negative and positive PDIV tests for the RC detector and the dipole antenna sensor.

The PDIV test indicated that PDIV occurred at voltages exceeding 9 kV, which serves as a reference for subsequent PD tests. Results from the dipole antenna revealed that negative PDIV appeared before positive PDIV. This observation aligns with the behavior of PD in needle-plate electrodes tested under air insulation. For positive PD, electrons originate from the SF6 gas, whereas for negative PD, electrons are emitted from the needle. Negative PD occurs first because the energy required to generate an initiating electron on the needle is lower than that required to produce an electron from SF6 gas. Consequently, the energy and voltage necessary to initiate negative PD are lower than those for positive PD.

Table 7. Negative and positive PDIV on the sensor

Sensor name	Positive PDIV (kV)	Negative PDIV (kV)
RC detector	10.3 kV	10.06 kV
Dipole Antenna	13.3 kV	10.06 kV

4.3.2. Waveform measurement

Based on previous PDIV testing, PDIV was observed at voltages exceeding 9 kV. For the waveform measurement, the partial discharge waveform was recorded at voltages above both the negative and positive PDIV values. Therefore, this PD test was conducted at a higher voltage level, specifically at 16 kV. The resulting waveforms from the dipole antenna, as detected by both the RC detector and the dipole antenna sensor, are presented in the Figure 7. The Figure 7 illustrates a dipole antenna, demonstrating that the waveform represents the simultaneous occurrence of RC waves and antenna waves. When PD occurs, the dipole antenna generates a greater number of waves compared to the RC detector.

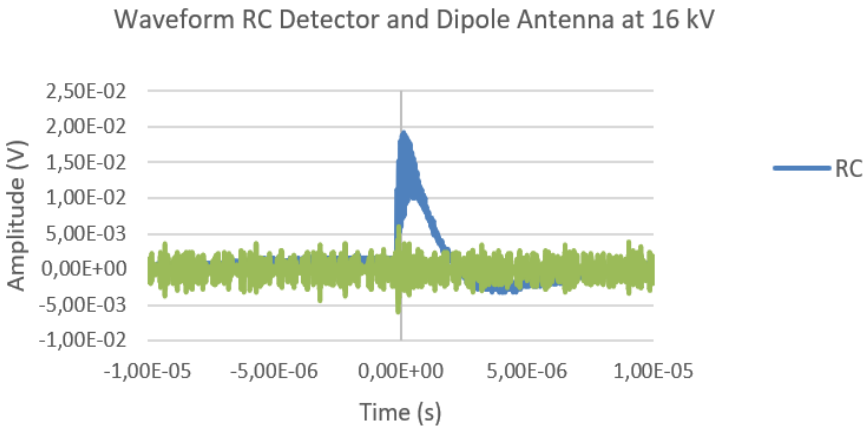

Figure 7. Waveform RC detector and dipole antenna at 16 kV

5. CONCLUSION

Dipole antennas designed for the UHF frequency range (300 MHz to 3 GHz) demonstrate that variations in design parameters have a significant impact on antenna performance. In previous research, A 66×15 mm dipole antenna yielded a bandwidth of 336 MHz, a return loss of -22.4 dB, and a resonance frequency of 1.3 GHz. Subsequently, after adjusting the length and width of the dipole antenna, the best results were obtained with a size of 35×40 mm. Modifying the antenna length to 35×40 mm results in a maximum bandwidth of 989 MHz and a return loss of -28.47 dB at a resonant frequency of 1.4 GHz. These findings indicate that the designed dipole antenna effectively detects partial discharge in GIS at a voltage level of 16 kV.

ACKNOWLEDGMENTS

This work was supported by the Ministry of Higher Education, Science, and Technology of Indonesia through Universitas Siliwangi.

REFERENCES

[1] S. Wang *et al.*, "Design of UHF-SHF sensor for the detection of GIS partial discharge," in *34th Electrical Insulation Conference, EIC 2016*, 2016, pp. 350–353, doi: 10.1109/EIC.2016.7548600.

[2] G. Robles, M. Sanchez-Fernandez, R. Albarracin Sanchez, M. V. Rojas-Moreno, E. Rajo-Iglesias, and J. M. Martinez-Tarifa, "Antenna parametrization for the detection of partial discharges," *IEEE Transactions on Instrumentation and Measurement*, vol. 62, no. 5, pp. 932–941, 2013, doi: 10.1109/TIM.2012.2223332.

[3] T. Rhamdhani, U. Khayam, and A. Zaeni, "Improving antenna performance by combining dipole and bowtie antenna for partial discharge measurement in gas insulated switchgear," *2022 IEEE International Conference in Power Engineering Application, ICPEA 2022 - Proceedings*, 2022, doi: 10.1109/ICPEA53519.2022.9744679.

[4] M. A. Darmaw, "Design, simulation, and fabrication of second, third, and forth order Hilbert antennas as ultra frequency partial discharge sensor," vol. 1, pp. 319–322, 2015.

[5] Y. Wang, Z. Wang, and J. Li, "UHF moore fractal antennas for online GIS PD detection," *IEEE Antennas and Wireless Propagation Letters*, vol. 16, pp. 852–855, 2017, doi: 10.1109/LAWP.2016.2609916.

[6] H. Luo, P. Cheng, H. Liu, K. Kang, F. Yang, and K. Liu, "Research on the UHF microstrip antenna for partial discharge detection in high voltage switchgear," in *2016 IEEE 11th Conference on Industrial Electronics and Applications (ICIEA)*, Jun. 2016, pp. 2273–2276, doi: 10.1109/ICIEA.2016.7603970.

[7] H. Andre and U. Khayam, "Design of new shape printed bowtie antena for ultra high frequency partial discharge sensor in gas-insulated substations," in *Proceedings - 2013 International Conference on Information Technology and Electrical Engineering: "Intelligent and Green Technologies for Sustainable Development", ICITEE 2013*, 2013, pp. 355–359, doi: 10.1109/ICITEED.2013.6676267.

[8] H. Andre, P. Emeraldi, A. Hazmi, E. P. Waldi, and U. Khayam, "Long bowtie antenna for partial discharge sensor in gas-insulated substation," in *International Conference on High Voltage Engineering and Power Systems, ICHVEPS 2017 - Proceeding*, 2017, vol. 2017-Janua, pp. 175–178, doi: 10.1109/ICHVEPS.2017.8225937.

[9] Y. M. Hamdani and U. Khayam, "Application of circular patch microstrip antenna (CPMA) for partial discharge detector in oil insulation," 2019, doi: 10.1109/ICHVEPS47643.2019.9011052.

[10] Y. M. Hamdani and U. Khayam, "Application of ultra-wideband double layer printed antenna for partial discharge detection," in *International Conference on Electrical Engineering, Computer Science and Informatics (EECSI)*, 2018, vol. 2018-Octob, pp. 373–378, doi: 10.1109/EECSI.2018.8752749.

[11] M. S. Habibi Daulay and U. Khayam, "Partial discharge pattern detected by new design partial discharge sensors," *Proceedings of the 2nd International Conference on High Voltage Engineering and Power Systems: Towards Sustainable and Reliable Power Delivery, ICHVEPS 2019*, 2019, doi: 10.1109/ICHVEPS47643.2019.9011079.

[12] A. A. Suryandi and U. Khayam, "New designed bowtie antenna with middle sliced modification as UHF sensor for partial discharge measurement," in *2014 International Conference on Smart Green Technology in Electrical and Information Systems (ICSGTEIS)*, Nov. 2014, no. November, pp. 98–101, doi: 10.1109/ICSGTEIS.2014.7038739.

[13] B. Wang, Y. Zhuang, and X. Li, "A novel dual ports antenna for handheld RFID reader applications," *Journal of Microelectronics, Electronic Components and Materials*, vol. 45, no. 2, pp. 125–131, 2015.

[14] Y. Chen, T. Zhao, Y. Wang, L. Zou, L. Zhang, and B. Yu, "Study on propagation characteristics of partial discharge electromagnetic wave in gas insulated switchgear," in *2019 IEEE 3rd International Electrical and Energy Conference (CIEEC)*, Sep. 2019, pp. 1170–1173, doi: 10.1109/CIEEC47146.2019.CIEEC-2019428.

[15] M. Horibe, "Performance comparisons between impedance analyzers and vector network analyzers for impedance measurement below 100 MHz frequency," *89th ARFTG Microwave Measurement Conference: Advanced Technologies for Communications, ARFTG 2017*, 2017, doi: 10.1109/ARFTG.2017.8000837.

[16] J. Verspecht, A. Stav, J. P. Teyssier, and S. Kusano, "Characterizing amplifier modulation distortion using a vector network analyzer," *2019 93rd ARFTG Microwave Measurement Conference: Measurement Challenges for the Upcoming RF and mm-Wave Communications and Sensing Systems, ARFTG 2019*, 2019, doi: 10.1109/ARFTG.2019.8739226.

[17] A. Darwish, S. S. Refaat, H. Abu-Rub, and G. Coapes, "A coplanar waveguide based antenna for partial discharge detection in gas-insulated switchgear," *3rd International Conference on Smart Grid and Renewable Energy, SGRE 2022 - Proceedings*, 2022, doi: 10.1109/SGRE53517.2022.9774181.

[18] K. Khotimah, U. Khayam, Suwarno, Y. Tai, M. Kozako, and M. Hikita, "Design of dipole antenna model for partial discharge detection in GIS," in *Proceedings - 5th International Conference on Electrical Engineering and Informatics: Bridging the Knowledge between Academic, Industry, and Community, ICEEI 2015*, 2015, pp. 186–191, doi: 10.1109/ICEEI.2015.7352493.

[19] Anon, "IEEE standard definitions of terms for antennas," *IEEE Transactions on Antennas and Propagation*, vol. AP-31, no. 6, 1983.

[20] R. K. Dhakad and M. V Kartikeyan, "Designing of patch antenna : A review," vol. 7109, 2014.

[21] G. Zhang, J. Tian, X. Zhang, J. Liu, and C. Lu, "A flexible planarized biconical antenna for partial discharge detection in gas-insulated switchgear," *IEEE Antennas and Wireless Propagation Letters*, vol. 21, no. 12, pp. 2432–2436, 2022, doi: 10.1109/LAWP.2022.3196176.

[22] L. Wang, Y. Shi, W. Guo, Z. Yang, and R. Li, "Research on partial discharge detection through ultra high frequency signal diffusing from GIS pouring aperture," in *Proceedings of the 30th Chinese Control and Decision Conference, CCDC 2018*, 2018, pp. 2207–2211, doi: 10.1109/CCDC.2018.8407493.

[23] T. Choudhury and G. R. Biswal, "SF6 density-and-viscosity sensing in gas insulated switchgear using MEMS resonator," 2017, doi: 10.1109/ICPEICES.2016.7853174.

[24] F. Guo, D. Hu, J. Li, X. Wu, X. Li, and S. Liu, "The partial discharge inception and breakdown voltage distribution of metal protrusion in SF6 gas," *2016 IEEE International Power Modulator and High Voltage Conference, IPMHVC 2016*, pp. 711–714, 2017, doi: 10.1109/IPMHVC.2016.8012851.

[25] D. Rajalakshmi, C. S. Sanoj, and N. Vijayaraj, "Design and optimization of printed dipole antenna for wireless sensor communication at 2.4GHz," 2013, doi: 10.1109/ICCCI.2013.6466262.

[26] M. Hassan, N. Elbeheiry, and S. S. Refaat, "Partial discharge inception voltage measurement for an artificially created void inside the solid dielectric," 2019, doi: 10.1109/SGRE46976.2019.9020695.

BIOGRAPHIES OF AUTHORS

Rian Nurdiansyah, S.T., M.T., is a lecturer in the Department of Electrical Engineering, Faculty of Engineering, Siliwangi University, Tasikmalaya City, Indonesia. He earned his Master's degree from the School of Electrical Engineering and Informatics, Bandung Institute of Technology (ITB), in 2019 with a specialization in high-voltage partial discharge diagnosis. In 2020, he joined Siliwangi University as a professional lecturer. Since then, he has been actively involved in research and community service, with academic interests focusing on high-voltage engineering, electrical insulation diagnostics, and the development of practical solutions to enhance electrical system reliability. He can be contacted via email at: riannurdiansyah42@unsil.ac.id.

Farradita Nugraha earned her S.T. degree in Electrical Engineering from the University of Indonesia (UI) and her M.T. degree in Electrical Engineering from the Bandung Institute of Technology (ITB). As a lecturer in the Department of Electrical Engineering, Faculty of Engineering, Siliwangi University, Tasikmalaya City, Indonesia. She is passionate about advancing the fields of high-voltage engineering and antenna technology. She can be contacted via email at farraditanugraha@unsil.ac.id.

Nadya Glaudira received her Bachelor of Applied Science degree in Telecommunication Engineering from POLBAN and her Master's degree in Telecommunication Engineering from Institut Teknologi Bandung (ITB). She is currently a lecturer in the Department of Electrical Engineering, Faculty of Engineering, Siliwangi University, Tasikmalaya City, Indonesia. Her research interests are in electromagnetic fields and antennas. She can be contacted at email: nadya.glaudira@unsil.ac.id.

Linda Faridah received her bachelor's degree in electrical engineering from the University of Education in Indonesia. She continued her studies with a master's program at the Bandung Institute of Technology (ITB) and is currently pursuing her doctorate at Yogyakarta State University. She is a lecturer in the Department of Electrical Engineering, Faculty of Engineering, Siliwangi University, Tasikmalaya City, Indonesia. Her interests include renewable energy, electric energy conversion, and electrical engineering. She can be contacted at email: lindafaridah@unsil.ac.id.